Optimizing holographic data storage using a fractional Fourier transform

Nicolas C. Pégard and Jason W. Fleischer*

Department of Electrical Engineering, Princeton University, Olden Street, Princeton, New Jersey 08544, USA
**Corresponding author: jasonf@princeton.edu*

Received March 31, 2011; revised May 20, 2011; accepted June 1, 2011;
posted June 2, 2011 (Doc. ID 145118); published July 1, 2011

We demonstrate a method to optimize the reconstruction of a hologram when the storage device has a limited dynamic range and a minimum grain size. The optimal solution at the recording plane occurs when the object wave has propagated an intermediate distance between the near and far fields. This distance corresponds to an optimal order and magnification of the fractional Fourier transform of the object. © 2011 Optical Society of America

OCIS codes: 070.0070, 090.0090, 210.0210.

Since holography captures the full wave function of an object, both its intensity pattern in real space and its spectral pattern in Fourier space are essential to the recording process. As these are dual, complete bases, it would not matter to an ideal holographic storage device (HSD) how the field itself is recorded. This can be seen most clearly in the simplest case: free-space propagation followed by interference with a plane wave, as the reference beam has no spatial information, while the propagation smoothly translates the wave function from the near-field (real-space) to the far-field (Fourier) basis. On the other hand, information storage capacity in real HSDs is limited by the dynamic range of the medium and the size of its recording elements (e.g., film grains or pixels). In the usual treatment of holographic recording, these limitations are expressed in terms of the diffraction efficiency of the hologram, e.g., via the exposure time and the angle of the reference beam, which determine the modulation depth and dominant spatial frequency of the recorded grating [1]. Often, however, it is desirable to keep these parameters fixed; the only degree of freedom remaining, then, is the distance of propagation between the object and the HSD. For a general object, it is reasonable to conclude that there is an optimal recording solution in which the interference happens between the near-field and far-field propagation. In other words, there is an optimal order α of the fractional Fourier transform (FrFT) [2] that most efficiently uses all of the available storage capacity.

FrFTs have been used in a variety of contexts. In its most basic form, an FrFT represents the propagation of a wave front through free space. More generally, the wave function in a linear optical system, such as a sequence of thin coaxial spherical lenses, can be represented by an FrFT up to a magnification factor [3]. Because of this, FrFTs have been used for signal processing [4] as well as all-optical signal encryption [5,6].

In the case of holographic storage, it is well known that a better signal-to-noise ratio is obtained when the HSD is placed closed to, but not at, the Fourier plane, as high DC peaks are avoided [7]. Theoretically, it has been shown for ideal but bandwidth-limited HSDs that applying an FrFT to a signal can improve its spectral uniformity and lead to better reconstruction of its hologram [8,9] (similar to the effect of diffusers but more quantitative and less sensitive to displacement and tilt [10]). Here, we generalize this result to HSDs with nonideal responses and propose a simple optical system that optimizes the recording and readout of holograms.

We consider the geometry shown in Fig. 1. Incident light reflects off of an object, creating a signal wave function $\mathcal{A}_{\mathrm{OBJ}}(x,y)$, which is recorded on a planar HSD located at a distance d along the propagation axis (z). To keep the system compact, we introduce a movable spherical lens between the object and HSD that can interpolate between the near-field and far-field wave functions. For generality, we allow the lens to have an adjustable focal length. The two degrees of freedom corresponding to the exposure time and the angle of the reference beam above are thus replaced by the location z_0 and focal length f of the lens. We note also that more general systems can be considered between the object and HSD, including nonlinear media [11], as long as the propagation is reversible.

With the lens in place, the beam to be recorded by the HSD is given by $\mathcal{A}_{\mathrm{WR}} = \mathcal{F}(\mathcal{A}_{\mathrm{OBJ}})$, where $\mathcal{F}(f_0, z_0)$ represents the Fresnel propagator of the system

$$\mathcal{F} = P^{(d-z_0)}\left[\exp\left(\frac{-ik(x^2+y^2)}{2f}\right)P^{(z_0)}\right]. \tag{1}$$

$P^{(x)}$ is the propagation operator through a length x of free space, and f is the focal length of the lens ($f \geq 0$ if the lens is convex). Using the standard hologram configuration, this signal interferes with a plane wave $We^{i\mathbf{k}_0\cdot\mathbf{x}}$, and the resulting intensity pattern records data onto the HSD:

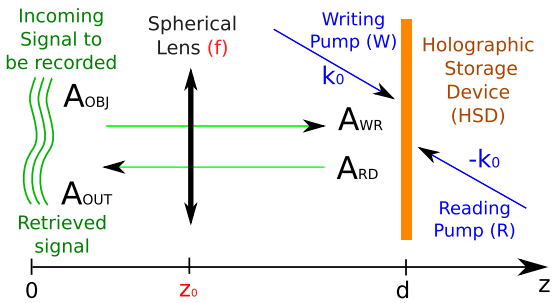

Fig. 1. (Color online) Reflection-type setup for quantification of holographic storage efficiency. In the optimal configuration, a thin spherical lens (position z_0, focal length f) minimizes the reconstruction error.

$$I = |\mathcal{A}_{\mathrm{WR}} + We^{i\boldsymbol{k}_0\cdot\boldsymbol{x}}|^2 = I_0 + 2\mathcal{R}e[W\mathcal{A}_{\mathrm{WR}}e^{i\boldsymbol{k}_0\cdot\boldsymbol{x}}]. \quad (2)$$

For faster computation of the signal propagation, we rewrite $\mathcal{F}$ as an FrFT [3] with fractional order α and magnification coefficient M:

$$[\mathcal{F}_M^{\alpha}(f)](u) = \int_{-\infty}^{\infty} K_{\alpha}\left(\frac{u}{M}, x\right) f(x)\mathrm{d}x, \quad (3)$$

$$K_{\alpha}(u,x) = \sum_{k=0}^{\infty} \psi_k(u)e^{-ik\alpha\pi/2}\psi_k(x), \quad (4)$$

where ψ_k is the kth Hermite–Gaussian function.

Readout of the hologram is performed by diffraction of a second, counterpropagating plane wave $Re^{i\boldsymbol{k}_0\cdot\boldsymbol{x}}$ on the recorded grating. W and R are the amplitudes of the pump beams for holographic writing and readout, respectively. This reflection-type hologram generates a phase-conjugated signal [12] that propagates backward through the system. This configuration provides a self-aligned, exact inverse transformation through the same optical device (lens), mitigating the non-shift-invariance of the FrFT. The analysis is similar for a transmission geometry, but in that case propagation on both sides of the HSD must be considered, requiring two separate systems to process the $\mathcal{F}$ and $\mathcal{F}^{-1}$ operations.

The interference pattern itself is recorded on a storage device, such as a CCD, piece of film, or photoresist. The response of the HSD is represented by an operator $\mathcal{H}$, which in general is a nonlinear function of $\mathcal{A}_{\mathrm{WR}}$, W, and R. Here, we consider two nonideal elements to the response: saturation and a minimum recording size. The first constraint arises from the limited dynamic range of the device, so that the response no longer increases above a certain value of light intensity. The second constraint arises from optical grain [13] or diffusion effects, e.g., film darkening or charge accumulation [14–16]. To model these in the simulations below, we define the operator $\mathcal{H}$ using the following two parameters: A characteristic diffusion length that is 1% of the transverse (x-axis) window length and a saturation coefficient by which the intensity of the recorded signal is limited to 50% of the maximum peak intensity observed in Fourier space.

The effects of these constraints are shown in Fig. 2. As a representative signal, we take a rectangular profile in intensity [Fig. 2(a)], with a sinc-like discrete Fourier transform [Fig. 2(b)]. For an accurate comparison, each beam is normalized so that the total intensity $\mathcal{I} = \int |\mathcal{A}|^2$ is conserved through holographic reconstruction steps: $\|\mathcal{I}_{\mathrm{OUT}}\| = \|\mathcal{I}_{\mathrm{OBJ}}\|$. Simulations of the Fresnel propagator for a direct-image hologram (FrFT order $\alpha = 0$) show that diffusion effects introduce soft edges in the reconstructed beam [Fig. 2(a)]. For a Fourier-recorded hologram (FrFT order $\alpha = 1$), diffusion effects leave the edges of the reconstructed beam sharp but introduce ringing. When saturation effects are taken into account [saturation level given by green line in Fig. 2(b)], the Fourier reconstruction suffers from significant errors in the low spatial frequencies [see Fig. 2(d)].

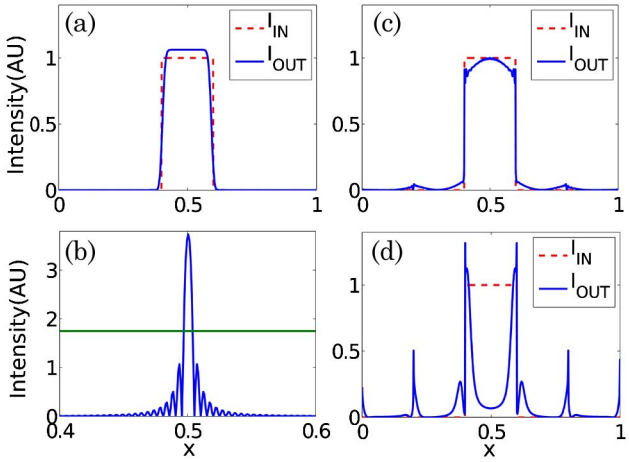

Fig. 2. (Color online) Input (dashed red) and readout (blue) simulation results for a rectangle signal. (a) Reconstruction of real-space hologram ($\alpha = 0$). Diffusion effects on the storage device induce reconstruction error on the edges. (b) Fourier transform of the rectangular signal. Green line shows the saturation level of the device. (c), (d) Reconstruction of Fourier-space hologram ($\alpha = 1$) after (c) diffusion and (d) saturation on the device.

To optimize the holographic readout, we assume that d, $\mathcal{A}_{\mathrm{OBJ}}$ and $\mathcal{H}$ are known and find the focal length f and placement z_0 of the lens that minimize the reconstruction error. If the HSD were ideal, we would have the operator $\mathcal{H} = \mathcal{I}d^{\star}$, the readout field $\mathcal{A}_{\mathrm{RD}} \approx \mathcal{A}_{\mathrm{WR}}^{\star}$, and the output field $\mathcal{A}_{\mathrm{OUT}} = \mathcal{A}_{\mathrm{OBJ}}^{\star}$ (aperture effects are neglected). As this is not possible, we want to solve

$$\min_{\mathcal{F}\in\mathcal{L}(\mathbb{R}^2)} \|\mathcal{I}_{\mathrm{OUT}} - \mathcal{I}_{\mathrm{OBJ}}\|, \quad (5)$$

where $\mathcal{I} = |\mathcal{A}|^2$, $\mathcal{A}_{\mathrm{RD}} = \mathcal{H}(\mathcal{A}_{\mathrm{WR}})$, and $\mathcal{A}_{\mathrm{OUT}} = \mathcal{F}^{-1}(\mathcal{A}_{\mathrm{RD}})$ so that $\mathcal{A}_{\mathrm{OUT}} = \mathcal{F}^{-1}\mathcal{H}\mathcal{F}(\mathcal{A}_{\mathrm{OBJ}})$.

In general, this optimization problem cannot be solved analytically because $\mathcal{H}$ is a nonlinear operator. We therefore resort to a numerical approach. In the case of an imaging system composed of one (or more) thin spherical lenses, Eq. (5) reduces to an optimization problem that depends only on two variables: $(f_0, z_0) \in \mathbb{R} \times [0, d]$ or equivalently $(M, \alpha) \in \mathbb{R}^+ \times [0, 1]$.

Hence, the optimization problem becomes

$$\min_{(\alpha,M)\in[0,1]\times\mathbb{R}^+} \||\mathcal{F}^{-1}\mathcal{H}\mathcal{F}(\mathcal{A}_{\mathrm{OBJ}})|^2 - |\mathcal{A}_{\mathrm{OBJ}}|^2\|. \quad (6)$$

There are a variety of choices for the norm, depending on the particular application. For example, it can be chosen to match the response of the human eye [17], to perform signal processing functions such as edge enhancement [18], or to optimize digital data storage by giving a higher penalty to localized errors [19]. Here, we will consider a standard $\mathcal{L}_2$ norm and evaluate the reconstruction error using $\|\mathcal{I}\| = [\int |\mathcal{I}(\boldsymbol{x})|^2 \mathrm{d}\boldsymbol{x}^2]^{1/2}$.

We note that, in general, the minimal reconstruction error is object-dependent (though a given solution may be approximately optimal for large classes of objects and measures). In Fig. 3 we show that the optimal configuration for the rectangle signal given in Fig. 2 corresponds to an FrFT of order $\alpha = 0.38$ and magnification

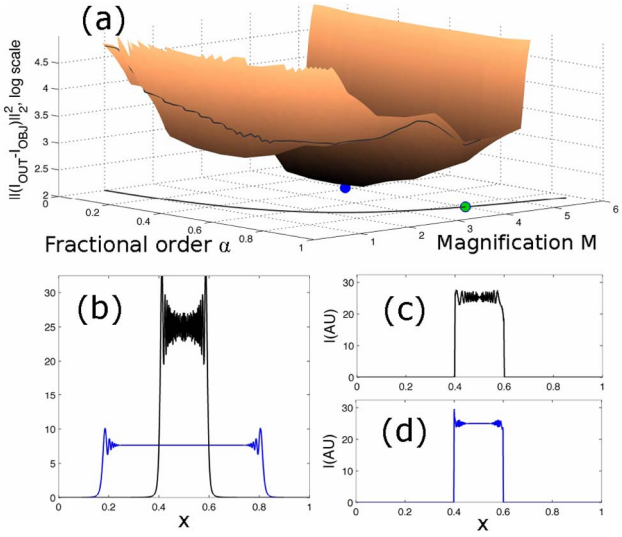

Fig. 3. (Color online) Reconstruction error of a rectangular signal. (a) Error as a function of fractional order α and magnification M, (b) field at recording device for optimal configuration for free-space propagation (black, narrow profile) and single-lens configuration (blue), (c), (d) reconstructed (readout) output fields for (c) free-space and (d) single-lens configurations.

$M = 3.9$ (blue dot). For comparison, the optimum for free-space propagation is given by $\alpha = 0.83$, $M = 4$ [for free space, $M = \sec(\alpha\pi/2)$]. The images on the HSD for free-space and single-lens propagation are shown in Fig. 3(b) with corresponding readouts shown in Figs. 3(c) and 3(d), respectively. We note that both of these optima occur at a significant distance from the Fourier plane.

We deduce from these results a convenient empirical method to quickly design efficient holographic storage experimental setups: the optimal fractional Fourier order corresponds to the one that expands any sharp edge along a distance that is comparable to the characteristic diffusion length, and the magnification factor is the one that extends this blurred version of the signal over the totality of the available holographic storage area.

In conclusion, we have demonstrated a method to optically increase the quality of holograms when the storage device has intrinsic limits in its recording ability. In particular, we used a single spherical lens with adjustable position and focal length to optimize devices with finite pixel size and dynamic range. As the lens modified beam propagation, the problem mapped to finding the ideal order and magnification of an FrFT. In general, the ideal value lies between the near-field and far-field wave functions, so that the peak intensity is below the saturation level and the smallest spatial scale is above the detector grain size. We considered the simplest case of a plane-wave reference beam and two limiting parameters of the recording device, but the main principle is general: by uniformly spreading both the intensity and the spectral distribution of the data to be recorded over all of the available holographic surface, we ensure the most efficient usage of the material's capacity.

This work was supported by the Air Force Office of Scientific Research (USAFOSR).

References

1. D. Psaltis, Science **298**, 1359 (2002).
2. D. Mendlovic and H. M. Ozatkas, J. Opt. Soc. Am. A **10**, 1875 (1993).
3. H. M. Ozaktas and D. Mendlovic, J. Opt. Soc. Am. A **12**, 743 (1995).
4. E. Sejdić, I. Djurović, and L. Stanković, Signal Process. **91**, 1351 (2011).
5. N. K. Nischal, J. Joseph, and K. Singh, Opt. Eng. **42**, 1583 (2003).
6. N. Singh and A. Sinha, Opt. Lasers Eng. **46**, 117 (2008).
7. H. Ramenah, P. Bertrand, E. H. Soubari, and P. Meyrueis, Opt. Lasers Eng. **28**, 589 (1996).
8. J. Sang-il, B. You-Seok, and L. Soo-Young, Opt. Commun. **198**, 57 (2001).
9. Z. Wang, G. Jin, Q. He, and M. Wu, Appl. Opt. **43**, 4896 (2004).
10. R. Jones and C. Wykes, *Holographic and Speckle Interferometry* (Cambridge University, 1983).
11. C. Barsi, W. Wan, and J. W. Fleischer, Nat. Photon. **3**, 211 (2009).
12. A. Yariv, Opt. Commun. **21**, 49 (1977).
13. W. H. Lee and M. O. Greer, J. Opt. Soc. Am. **61**, 402 (1971).
14. K. Buse, Appl. Phys. B **64**, 273 (1997).
15. J. Sha, J.-K. Lee, S. Kang, V. M. Prabhu, C. L. Soles, P. V. Bonnesen, and C. K. Ober, Chem. Mater. **22**, 3093 (2010).
16. K. Buse, A. Adibi, and D. Psaltis, Nature **393**, 665 (1998).
17. A. M. Eskicioglu and P. S. Fisher, NASA Conf. Publ. **3191**, 49 (1993).
18. J. Feinberg, Opt. Lett. **5**, 330 (1980).
19. G. W. Burr, J. J. Ashley, B. Marcus, C. M. Jefferson, J. A. Hoffnagle, and H. J. Coufal, Proc. SPIE **3468**, 64 (1998).